# Frequency dependence of elastic and attenuation properties of cracked media: Ultrasonic modeling studied

J. J. S. de Figueiredo*(Unicamp-Brazil and University of Houston), Robert R. Stewart (University of Houston), Nikolay Dyaur (University of Houston), J. Schleicher (INCT-GP and Unicamp-Brazil), Bode Omoboya (University of Houston), Robert Wiley (University of Houston) and Anoop William (University of Houston).



## Abstract

**Anisotropic cracked media have been widely investigated in many theoretical and experimental studies. In this work, we perform ultrasonic surveys to investigate the influence of source frequency on elastic parameters (the Thomsen parameter $\gamma$ and shear-wave attenuation) of fractured anisotropic media. Under controlled conditions, we prepared anisotropic models containing penny-shaped rubber inclusions in a solid epoxy resin matrix with crack density that ranges from 0 to 6.2 %. Two of the three models have 10 layers and the last has 17 layers, the number of uniform rubber inclusions per layer was from 0 up to 100. S-wave splitting measurements have shown that scattering effects are more prominent in models where the crack aperture to seismic wavelength ratio ranges from 1.3 to 13.3 than other models where the ratio was varied from 2.3 to 23. The model with large cracks gave a magnitude of attenuation 3 times higher compared with another model that had small inclusions. These results indicate acoustic scattering, attenuation (intrinsic and apparent), and velocity dispersion directly interfere in shear wave splitting, which in turn is a function of crack aperture and source frequency.**

## Introdution

Physical modeling is a useful tool to simulate conditions present in the field and parameters in numerical methods. Previous experiments conducted by Assa'd et al. (1993) and Wei (2004) established an experimental relationship between crack density and shear velocity based on theoretical predictions by Hudson (1981). Other theoretical and experimental studies carried out by Marion et al. (1994) and Melia et al. (1984) showed the influence of short and long wavelengths in stratified media.

In anisotropic cracked media, the frequency response is influenced by size of heterogeneities. To better understand the influence of frequency on cracked materials, we conducted a series of experiments aimed at extending previous approaches by using a shear-wave source with different frequencies. In this work, we carried out experiments, on a reference model (without inclusions) and three other models with different sizes of inclusion and thereby simulated different crack densities. The shear-wave profiles were measured using three different S-wave transducers with dominant frequencies from 0.09 MHz, 0.450 MHz and 0.840 MHz. In this arrangement, shear-wave splitting was observed with different magnitudes as a function of frequency. Our results show that effects associated with scattering and apparent attenuation (Görich and Müller, 1987) interfere directly with shear wave splitting, which in turn is related to crack density. Furthermore, we observed that the anisotropic parameter $\gamma$ (Thomsen, 1981) varies with frequency and size of crack. The quantification of attenuation has been determined using the drift-time correction method (Stewart et al., 1984).

## Experimental procedure

The construction of the cracked samples as well as the ultrasonic measurements were carried out at the Allied Geophysical Laboratories (AGL) at the University of Houston.

***Model preparation*:** In controlled conditions, we made three cracked models (M2, M3 and M4) with different crack densities and an uncracked model (M1) for reference. The pictures of all models are shown in Figure 1. The model M4 has five different points that can be analyzed. The same distance between layers (0.5 cm for M2 and M4 and 0.25 cm for M3) was ensured by using the same volume of epoxy resin poured for each layer. Each layer with inclusions was added to the model and air was extracted using a vacuum pump so as to avoid inhomogeneities in the epoxy resin. The crack density ε in the cracked models was determined using the following equation,

$$\varepsilon = \left( \frac{N \pi r^2 h}{V} \right) \qquad (1)$$

where *N* is total number, *r* is radius, *h* is thickness of inclusions (aperture of cracks), and *V* is volume of model. Equation (1) is a modification of Hudson's (1981) relation for crack density estimation. The ratio of compressional wave velocity between solid epoxy and neoprene was ~1.5 and for solid epoxy and silicone rubber was ~2.25.

S-wave velocity in rubber was difficult to determine because of low shear modulus of this material. The sizes of the included rubber cracks in each model are displayed in Table 1.

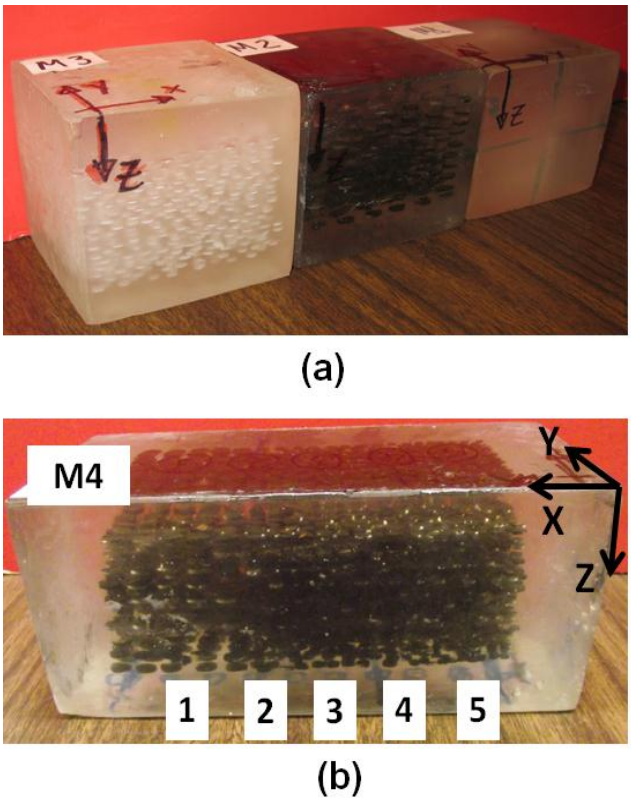


*Figure 1: Reference model M1 (uncracked) and cracked models M2, M3 and M4. All wave measurements were made in Y direction.*

***Ultrasonic measurements***:The ultrasonic measurements were carried out using the Ultrasonic Research System at AGL using the pulse transmission technique. The sampling rate per channel for all experiments was 10 MHz. Figure 2 (a) shows a device developed for recording S-wave seismograms.

| Model | Crack density (%) | Measure distance (cm) | Number of Layers | [Diameter] (cm) – [aperture] (cm) of cracks | Number of cracks per layer | Aspect –ratio |
|---|---|---|---|---|---|---|
| **M1** | Isotropic | 7.31 ± 0.02 | 0 | 0 | 0 | 0 |
| **M2** | 4.5 | 7.29± 0.02 | 10 | [0.7] - [0.091] | 36 | 0.13 |
| **M3** | 3.8 | 7.32 ± 0.02 | 17 | [0.4] - [0.051] | 90 | 0.12 |
| **M4-1** | 6.2 | 7.64 ± 0.02 | 10 | [0.7] - [0.091] | 30 | 0.13 |
| **M4-3** | 5.2 | 7.74 ± 0.02 | 10 | [0.44] -[0.091] | 80 | 0.20 |
| **M4-5** | 3.8 | 7.74 ± 0.02 | 10 | [0.32] - [0.091] | 100 | 0.28 |

***Table 1:*** *Physical parameters of models M1, M2, M3 and M4.*

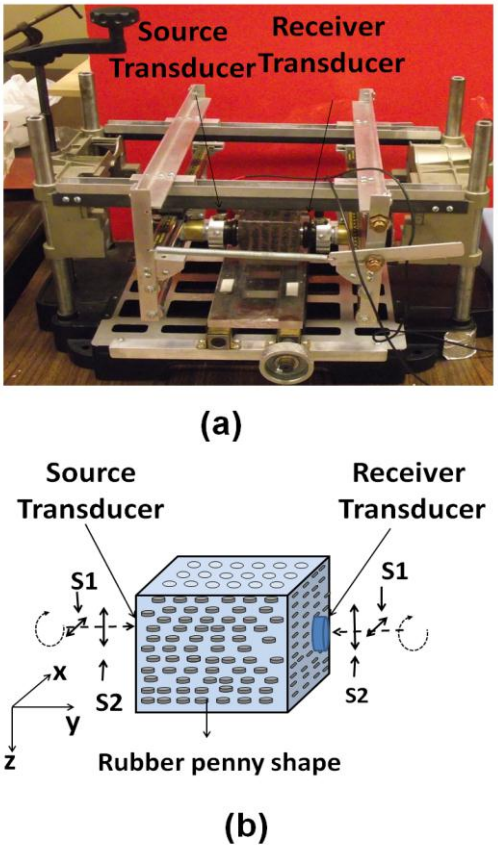


*Figure 2: (a) Device developed for S-wave polarization rotation. (b) Sketch of experiment used for seismogram records.*

The source and receiver transducers were arranged on opposing sides of the model with initial shear-wave polarization parallel to the cracks. Changes in polarization were achieved by rotating both transducers 10 degrees each time until polarization was again parallel (i.e., 0 to 180 degrees) to the XZ plane (see Figure 2b). In total, 19 traces were recorded in each seismic section. The polarizations 0 and 180 degrees correspond to the fast S-wave ($S_1$) and 90 degrees corresponds to the slow S-wave ($S_2$). The delay time in all S-wave transducers was 0.27 *μs.* For velocity computation, the delay time was subtracted from the observed arrival time. The accuracy of picking time was ± 0.1 *μs,* which allows to estimate the error in velocity of ± 0.3%.

**Models M1, M2 and M3- Results**

Shear-wave splitting was observed for all frequencies in models M2 and M3. The magnitude of this birefringence also appears to depend on the frequency of the source. Figure 3 shows seismograms from models M1, M2 and M3 with three different frequencies. The isotropic model (M1) shows uniform first arrivals with $S_1$ ($0^{\circ}$ and $180^{\circ}$) and $S_2$ ($90^{\circ}$) for all kind of sources used. In model M2, for low and intermediate frequencies (0.09 MHz and 0.450 MHz), the splitting observed between the fast and slow shear

waves was 7.0 μs and 5.6 μs respectively. In model M3, the values of splitting were 4.0 μs and 3.6 μs for low and intermediate frequencies respectively. In the case of the high frequency measurement, model M2 (see Figure 3c) shows inconsistent fast and slow shear wave arrivals. This can be attributed to the fact that the pulse wavelength is of the same order as that of the crack aperture. Similarly, due to the small ratio between wavelength and crack aperture, the model M3 for source frequency 0.840 MHz presents a splitting equal to 2.5 μs.

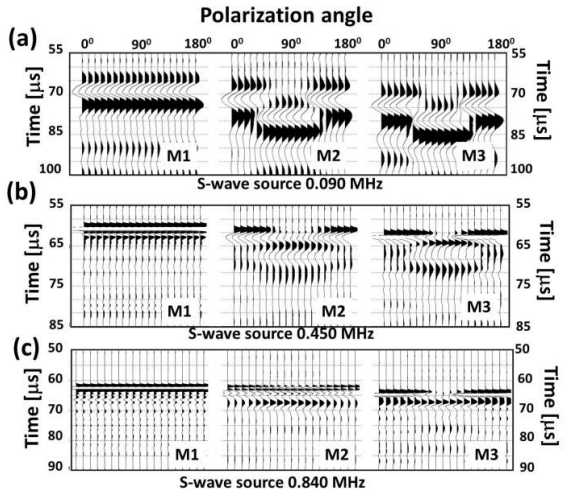


*Figure 3: S-wave seismograms as function of change in polarization from 0° to 180° for models M1 (isotropic), M2 (ε = 4%) and M3 (ε=3.5 %) with three different frequency transducers: (a) 0.090 (b) 0.450 and (c) 0.840 MHz.*

Figures 4 shows the Fourier spectra obtained for model Figures 4 shows the Fourier spectra obtained for model M1. As can be observed, the waves are more strongly attenuated in epoxy resin for high frequencies where the dominant frequency is shifted from 0.840 MHz (source frequency) to 0.51 MHz (frequency response). In model M2, the ratio of wavelength to crack aperture ranges between 1.3 to 13.3 and hence effects associated with scattering as well as effective media are expected. Figure 5 shows the Fourier spectra for the model M2. As it is observed in Figure 3 (a), before the first arrival some ringing effects can be noted. This feature is followed by a second peak shown in Figure 5 (a). Important aspects to note here are a strong shift of the dominant frequency with respect to the dominant frequency of the source and a pronounced second peak for $S_2$ polarization. This means that the polarization appears to be more affected by crack aperture. Figure 5 (b) and (c) do not exhibit the high second peak. However strong shifts of the dominant frequencies of the $S_1$ and $S_2$-wave polarizations can be noted. For better comparison, we applied a band-pass filter of 1-5-35-40 Hz to the scaled seismogram (upscaled by 10000) shown in Figure 3 (c)–M2. The part of the seismogram associated with acoustic scattering due to high frequency is shown in Figure 6. We note a shear-wave splitting with a magnitude of 1.8 ms in Figure 6 (b), which was not observed before. On the other hand, the seismic section associated with the peaks at 0.75 MHz and 0.82 MHz can be observed in the Figure 6 (c).

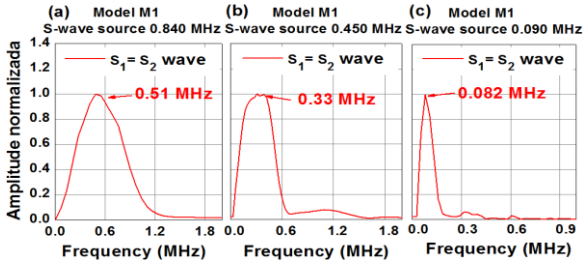


*Figure 4: Frequency spectra response for model M1 using S-wave sources (a) 0.840, (b) 0.450 and (c) 0.090 MHz.*

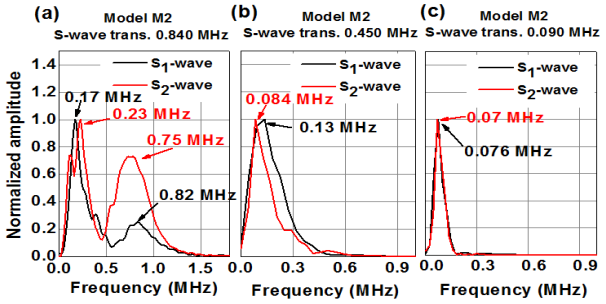


*Figure 5: Frequency spectra response for model M2 using S-wave sources (a) 0.840, (b) 0.450 and (c) 0.090 MHz.*

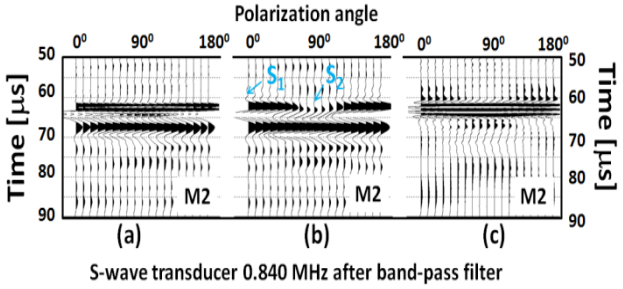


*Figure 6: (a) S-wave seismogram for model M2 (b) The same data after application of band-pass filter 1-5-35-40 Hz (S-wave splitting is 1.8 ms). (c) High-frequency section after subtraction of (a) from (b).*

Figure 7 shows the frequency spectra of model M3 for the $S_1$ and $S_2$-polarizations. Compared to model M2, M3 does not produce a second peak in the high frequency range. However, as can be noted, the shift in frequency associated with the perpendicular polarization ($S_2$) is more prominent. The observed delay between shear waves for model M3 is 3.0 μs (see Figure 3(c)-M3) and pulse wavelength to crack aperture ratio ranges from 1 to 2.3. This explains why there is less acoustic scattering and consistent time arrivals as compared to model M2. The relationships between velocities $V_{S1}$ and $V_{S2}$ and source transducer frequency are shown in Figure 8. Figure 8(d) shows Thomsen's anisotropy parameter γ as a function of source frequency. The parameter calculation was based on the following equation (Thomsen, 1986):

$$\gamma = \frac{1}{2}\left(\frac{V_{s1}^{\ 2}}{V_{s2}^{\ 2}} - 1\right) \qquad (2)$$

where $V_{S1}$ and $V_{S2}$ are the velocities of the fast and slow shear wave in cracked media.

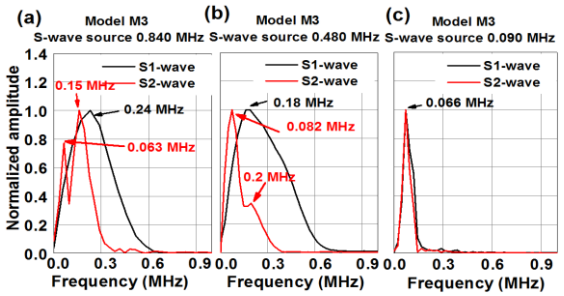


*Figure 7: Frequency spectra response for model M3 using S-wave sources (a) 0.840, (b) 0.450 and (c) 0.090 MHz.*

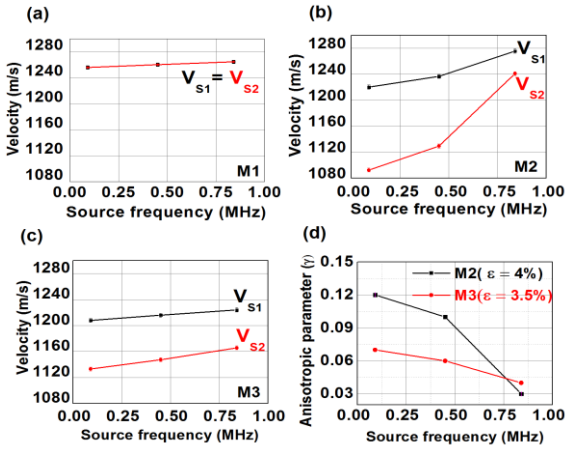


*Figure 8: Velocity plots for models M1 (a), M2 (b) and M3 (c) as a function of frequency. (d) Anisotropic parameter.*

We can conclude from these velocity results that the magnitudes of shear-wave splitting appear to depend on frequency and apparent attenuation due to acoustic scattering. This splitting is more pronounced at the lowest frequency (0.090 MHz) for all cracked models whereas the limit is more near the one for effective media for both models. We can infer from Figure 8(d) the relationship between seismic frequency (and wavelength) and crack aperture. At long wavelengths (low frequency), this anisotropy percentage is higher.

**Shear-wave attenuation measurement**

There are many difficulties that are encountered in the laboratory and field to accurately measure an attenuation value. Effects related to the near-field, spherical divergence, boundaries, reflectors, and scattering are factors that change the amplitude of a seismic trace. To avoid these effects, we used a method that basically depends on the time shift observed in the first arrival measurements in two or more different frequency sources and frequency response of medium for attenuation calculation. This method, which does not require any amplitude ratio approach (like, e.g., the spectral ratio), was established by Stewart et al. (1984). Mathematically, the delay time equation can be written as

$$t_{delay} = \frac{l \ln\left(w_j / w_i\right)}{\pi Q V(w_j)} \qquad (3)$$

where $l$ is length of wave propagated in cracked media (our case length in Y direction), $\omega_j$ is the dominant frequency response of medium using low frequency source, $\omega_i$ is the is the dominant frequency response of medium using high frequency source , $V(\omega_j)$ is a velocity for frequency $\omega_j$ and Q is quality factor. In our case, the index $j$ can be 2 or 3. For $j$=2, the frequency response acquired using a shear-wave source is 0.450 MHz and when $j$=3 it is 0.840 MHz. Here, index $i$ is always 1, which corresponds to frequency responses using the shear-wave transducer with a frequency of 0.090 MHz. The Table 2 shows the values of all frequencies responses for models M1, M2 and M3 as well as shift-time between the frequency responses ($w_3$, $w_1$) and ($w_2$, $w_1$). From equation (3) we calculated $Q^{-1}$ using the values of Table 1 and the velocities shown in Figure 8. The length of wave propagation was also shown in Table 1. As mentioned in the last section, the $S_2$ polarization is more influenced than the $S_1$ polarization for large and small crack aperture. Nonetheless, the attenuation is more pronounced for M2 for both S1 and S2 polarizations. This can be seen in Figure 9.

| | Frequencies(MHz) | | | Shift-time (ms) | |
|---|---|---|---|---|---|
| Model | w1(S1,S2) | w2(S1,S2) | w3(S1,S2) | \|t(w3)- t(w1)\| (S1,S2) | \|t(w2)-t(w1)\| (S1,S2) |
| M1 | (0.082,0.082) | (0.377,0.377) | (0.514,0.514) | (0.4,0.4) | (0.2,0.2) |
| M2 | (0.076,0.07) | (0.13,0.18) | (0.17,0.24) | (1.8,7.2) | (0.8,5.0) |
| M3 | (0.073,0.067) | (0.18,0.08) | (0.24,0.156) | (0.8,1.8) | (0.4,0.7) |

*Table 2: Frequencies and drift-time for models M1, M2 and M3 respectively the shear-wave polarizations $S_1$ and $S_2$.*

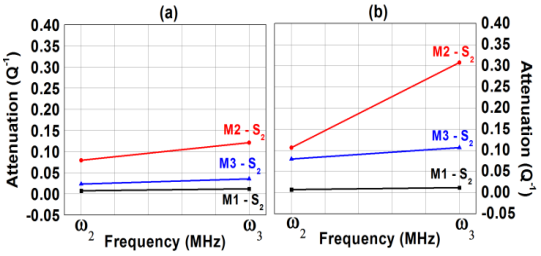


*Figure 9: Attenuation $Q^{-1}$ for models M1, M2 and M3 respectively for the shear-wave polarizations $S_1$ and $S_2$.*

**Model M4 - Anisotropic parameter γ**

Figure 10 shows the velocity of shear-waves ($S_1$ and $S_2$ obtined) for model M4 using frequencies source 0.090,

0.450 and 0.840 MHz. The model M4 has three different aspect-ratios (0.13, 0.20 and 0.28) but has the same aperture (0.091 cm). As we can see, the S-wave splitting has strong dependency on the size and density of the cracks. In Figure 9 (a) and (b), where the long wavelength is dominant, the anisotropic parameter decreases with reduced crack density. On the other hand, in the high frequency limit the lower crack density with small crack size shows an increase in magnitude of anisotropy parameter $\gamma$. Thus, we can state that the size of the cracks is more influential than the aperture in che case of a high frequency source.

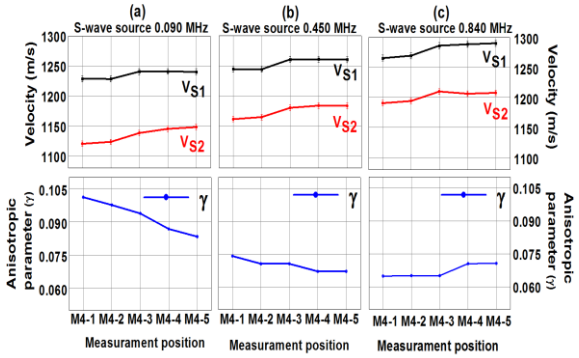


*Figure 10: Velocities plots for five different points in model M4 and the respective anisotropic parameter $\gamma$ associated with these velocities for S-wave source transducers (a) 0.840 MHZ, (b) 0.450 and (c) 0.090 MHz*.

## Conclusions

This experimental study has investigated the influence of frequency in anisotropic media containing aligned cracks. The results show that S-wave splitting directly depends on the frequency of source and the crack aperture. With low frequencies, this splitting is more conspicuous. A decrease in velocity was noted when the frequency of the source was decreased and the observed dispersive effects were more pronounced. The scattering effect was more pronounced when the crack aperture had the same magnitude as the source wavelength. Furthermore, apparent attenuation was more pronounced when the shear-wave polarization was perpendicular to the crack plane.

## Acknowledgments

This work was made possible by the Allied Geophysics Laboratories financial support. The authors are grateful to Dr. Leon Thomsen for his advice. The first author wishes to thank CAPES and CNPq from Brazil by the scholarship (contract # 201461/2009-9).

## References

Assa'd, J. M., Tatham, R. H., and McDonald, J.A. , 1992, A physical model study of microcrack-induced anisotropy, Geophysics, 57, 1562-1570.

Gorich, M., and Muller, G., 1987, Apparent and Intrinsic Q. The One-dimensional Case, J. Geophys. 61, 46–54.

Hudson, J. A., 1981, Wave speeds and attenuation of elastic waves in material containing cracks. Geophys. J. R. Ast. Soc., 64, 133-150.

Marion, D., Mukerji, T., and Mavko, G., 1994, Scale effects on velocity dispersion: From ray to effective medium theories in stratified media, Geophysics 59, 1613-1619.

Melia, P. J., and Carison, R.L., 1984, An experimental test of P-wave anisotropy in stratified media. Geophysics, 49, 374-378

Stewart, R.R., Huddleston, P. D., and Kan, T. K., 1984, Seismic versus sonic velocities: A vertical seismic profiling study. Geophysics, 49, 1153-1168.

Thomsen, L., 1986, Weak elastic anisotropy, Geophysics, 51, 1954-1966.